IEEE Access
Multidisciplinary | Rapid Review | Open Access Journal

IEEE POWER & ENERGY SOCIETY SECTION

Received 9 December 2025, accepted 2 January 2026, date of publication 12 January 2026, date of current version 21 January 2026.

Digital Object Identifier 10.1109/ACCESS.2026.3653346

RESEARCH ARTICLE

Voltage Magnitude and Voltage Stability Margin Optimization Through Allocation and Sizing of SVCs via VNS Algorithm

CESAR E. C. CARRIÓN, WANDRY R. FARIA, ELLEN C. C. DE SOUZA, RODRIGO A. RAMOS, (Senior Member, IEEE), EDUARDO N. ASADA, (Senior Member, IEEE), AND BENVINDO R. PEREIRA JUNIOR

São Carlos School of Engineering, University of São Paulo, São Carlos 13566-590, Brazil

Corresponding author: Cesar E. C. Carrión (cesarcuro.cc@usp.br)

This work was supported in part by the Research Centre for Greenhouse Gas Innovation (RCGI), based at the University of São Paulo (USP) under Grant 23.1.8493.1.9; in part by São Paulo Research Foundation (FAPESP)—São Paulo Research Foundation under Grant 2020/15230-5; in part by the TotalEnergies; in part by the Coordination for the Improvement of Higher Education Personnel (CAPES) under Grant 001; and in part by Brazilian National Council for Scientific and Technological Development (CNPq) Grant 408464/2023-2.

ABSTRACT An effective approach to address challenges in voltage regulation is the allocation of equipment that provide fast-responding reactive power support to the power system. This paper presents an optimization approach for the strategic allocation of Static VAR Compensators (SVCs), aiming to enhance voltage magnitude and stability margin. The proposed methodology incorporates Voltage Severity Index (VSI) and Voltage Security Margin (VSM) analysis to ensure operational reliability and prevent voltage collapse under different system conditions. The optimization model, formulated as a mixed-integer non-linear problem, considers key SVC operational characteristics, including the slope of the Q/V operating curve, reactive power capacity, the voltage magnitude reference value for the controlled bus, and the possibility of remotely controlling the voltage magnitude of a specific bus. Given the complexity of the problem, a Variable Neighborhood Search (VNS) algorithm was developed and tailored to efficiently explore the solution space and determine high-quality strategies for SVC placement and sizing. Simulation results on a 107-bus test system demonstrate the effectiveness of the proposed approach in mitigating voltage violations and enhancing stability margins for multiple operational conditions. The solution found by the proposed algorithm enhances the power system's performance by 54% VSI-wise and up to 540% VSM-wise.

INDEX TERMS Contingency management, metaheuristics, optimization models, power system stability, power transmission, reactive power control, static VAr compensators.

I. INTRODUCTION

The increasing demand for electricity and the integration of renewable energy sources have made Electric Power System (EPS) more susceptible to fluctuations in generation and demand [1]. These variations can compromise the security of EPS, leading, in extreme cases, to system collapses, as evidenced by blackouts in several countries [2], [3], [4]. In some cases, events of this nature are caused by a lack of reactive power support, leading to the phenomenon known as voltage collapse. Given the possible scenario of low reactive power support and high power injection uncertainty due to renewable sources, some regulatory agencies and Transmission System Operators (TSOs) adopt a conservative stance towards the EPS operation. Under such a risk-averse operation, scenarios involving the power curtailment in renewable-based power plants become more frequent, which is the current reality of the Brazilian Interconnected Power System (BIPS). In the context of the BIPS operation, scenarios in which resources for voltage control may be exhausted are usually observed for the Northeastern region, where most wind power plants are located and the local demand is low when compared to the generation availability [5]. As a result, most curtailment

The associate editor coordinating the review of this manuscript and approving it for publication was Emilio Barocio.

events in the BIPS occur at the Northeastern subsystem. It should be mentioned that this is not an issue endemic to the BIPS. Hence, the strategic planning of allocating devices that provide reactive power support for voltage regulation has emerged as a crucial element for the secure and efficient operation of any modern EPS.

Shunt-connected Flexible AC Transmission System (FACTS) devices rely on power electronics to quickly and precisely react to voltage changes in the EPS by injecting or absorbing reactive power. By doing so, these devices are extremely effective in enhancing the EPS' voltage magnitude profile and stability regardless of the power system's operational condition (normal or under contingency) and for both steady-state and dynamic time-frames [6]. Although the operation of these FACTS devices may enhance the performance of the EPS as a whole, the equipments operate based on a limited amount of measurements from the EPS. Hence, it is important to allocate the devices at strategic locations so that system-wide enhancement is attained by regulating the voltage of these specific buses.

The STATCOM stands out among the shunt-connected FACTS devices for its broad application and proven efficiency in improving dynamic and transient stability in renewable-integrated power systems when properly allocated, as demonstrated in recent studies [7], [8]. Nonetheless, the Static VAR Compensator (SVC) is still one of the most widely used FACTS devices due to its easier installation (in comparison to series-connected devices) and relatively low acquisition costs (in comparison to other shunt-connected FACTS devices such as the STATCOM). Its operating principle allows for continuous voltage modulation within an operational range through the injection or absorption of reactive power, in contrast with the traditional shunt elements installed in the system (i.e., capacitor and inductor banks), which provide discrete voltage control [1].

The specialized literature includes various methodologies for optimizing the allocation and sizing of SVCs in transmission systems. The objectives of these studies vary, ranging from power loss minimization to loading margin maximization. Given the binary nature of the allocation problems and the non-linear constraints associated with the formulation of the EPS operation, off-the-shelf solvers may not be efficient to tackle large-scale problems. Thus, most of the proposals addressing this problem available in the literature employ metaheuristic-based techniques to place and size FACTS devices. Moreover, some authors address only the allocation of the sizing problem, instead of tackling both simultaneously. For instance, in [1], a Whale Optimization Technique (WOA) is applied to determine the best size of FACTS devices, while [9] employs a Artificial Bee Colony (ABC) to optimize their placement. The two optimization models adopt different objective functions; nonetheless, both are incomplete as only one of the main aspects of the SVC, namely location and capacity, are addressed by the authors. In contrast, the authors of [10] and [11] propose Genetic Algorithms (GAs) that simultaneously tackles both the placement and sizing of multiple FACTS devices aiming to maximize system loading margin, which is an indicator of the Voltage Stability Margin (VSM).

Another branch of papers explore the application of mathematical programming instead of metaheuristic-based algorithms to optimize the allocation of FACTS devices. In [12], a Mixed Integer Linear Programming (MILP) formulation using Line Flow Based (LFB) equations is developed to optimize SVC placement, maximizing loadability while minimizing reactive compensation with a penalty term. Similarly, [13] proposes a Second-Order Cone Programming (SOCP) model to minimize active power losses and enhance voltage profiles under load uncertainties across multiple scenarios, utilizing convex reformulations of the LFB equations. In [14], an SOCP-based approach is employed to optimize SVC allocation by minimizing active power losses in a single load scenario, leveraging a convexified AC branch flow model. While these methodologies may offer computational advantages compared to evolutionary algorithms, they depend heavily on simplified power flow models and relaxation parameters, which may fail to capture the full complexity of power system behavior.

Moreover, all of the approaches (metaheuristic and mathematical programming) mentioned thus far neglect contingency scenarios. Thus, although the EPS performance is enhanced for the normal operation, there is no analysis regarding abnormal events, which could possibly benefit the system's resilience if taken into account by the optimization process.

In this context, the authors of [15] and [16] build upon the proposals mentioned in the previous paragraph by 1) actually calculating the VSM using a Continuation Power Flow (CPF) routine and 2) taking into account outage contingencies. In both papers, the authors verify the effects of N-1 contingencies and identify the most sensible bus voltage-wise under the most severe contingency. Then, an SVC is strategically placed at this critical bus and the sizing is determined by the optimization process. It should be highlighted that, in both methods, the authors address the enhancement of a single bus voltage magnitude considering a single contingency scenario. As a result, these approaches may be insufficient to avoid voltage collapse when considering, for example, the second most critical event, which in many cases may have a higher probability of occurrence.

Other proposals, such as those presented in [17] and [18], represent the optimization problem as instances of mixed-integer non-linear programming. Given the lack of reliable commercial solvers, the authors employ the Benders decomposing technique to separate the original problem into a mixed-integer main problem, which address the SVC allocation, and a non-linear subproblem, that represents the EPS operation for a given allocation decision. The authors formulate the optimization problem to enhance the performance of EPSs under both normal operating conditions and multiple contingency scenarios, instead of a single event as considered in the papers listed in the previous paragraph.

Despite the advantages over the other formulations listed thus far, these proposals feature two major drawbacks. Firstly, the subproblems present non-linear formulations; therefore, the Benders decomposition may not always converge and, when it does, it may not be the optimal solution nor will the technique always converge to the same solution. Additionally, these studies tend to overlook or oversimplify the operational characteristics of SVCs, which will be presented in the following section. For instance, SVCs are modeled as variable susceptances constrained only by their rated capacity. Thus, the susceptance value is optimized to enhance the VSM based on system-wide electrical variables. In reality, the SVC susceptance changes based on the voltage of a single bus, which must be kept at a pre-defined value, following a linear Q/V curve (if the voltage is within the control limits).

More recent approaches, such as [19] and [20], focus on the allocation of capacitor banks and STATCOMs to increase voltage support during contingencies. The effectiveness of the allocated devices is assessed primarily from a dynamic perspective, albeit steady-state constraints are also considered. The voltage support provided by the newly allocated devices reduces undervoltage events during the transient period after a contingency; as a result, inverter-based generators, such as wind and solar, are less likely to be disconnected, which could trigger a cascading event. The authors of [21] address the problem from a steady-state perspective; similar to [17] and [18], they propose allocating capacitor banks (shunt and series) and SVCs to maximize the system loadability. Given the complexity of the resulting optimization problem, the authors employ a GA to address it. Nonetheless, it should be mentioned that contingency events are not considered in the optimization process. Thus, the new devices enhance the system loadability under normal operation, not necessarily under contingency events. Moreover, the reactive power of the FACTS devices is not modeled to respond to the voltage magnitude. Although such consideration enhances overall system performance, as it results from centralized optimization that considers every aspect of the network, in reality, these devices operate with limited system measurements and do not always benefit the system as a whole.

Finally, [22] presents a formulation for the optimal allocation of reactive power sources to ensure the absence of voltage magnitude issues even when the system operates under contingencies. It must be highlighted that these authors enforce that the non-automated controls cannot be changed in response to contingencies, i.e., a preventive mode constraint, which is not featured in the papers mentioned thus far. Nonetheless, the operational constraints of SVCs and STATCOMs require that the voltage magnitude at their connection point be maintained constant regardless of the system's operational condition (i.e., normal or under contingency). If this constraint cannot be held, the allocation is infeasible. Since voltage limits are imposed on every bus, the capacity of the FACTS devices allocated to critical buses must be increased to maintain the specified voltage during contingency events. Although the devices' formulation can model their operation in real-world conditions, it is a very conservative approach, since droop-based Q(V) curves can be used to model the response of real SVCs and STATCOMs, thereby reducing the installed capacity. Furthermore, the authors do not investigate the effects of the allocation on the system's loadability.

Based on the literature review presented in this section, one can identify a couple of gaps in the existing proposals. In this paper, we address some of them by introducing a novel optimization model for the allocation and sizing of SVCs in EPSs. In comparison with the models proposed in [17], [18], [19], [20], [21], the SVC representation employed in this paper is more accurate since the reactive power is expressed as a function of the voltage magnitude, which must be kept close to a reference value. It should be stressed that the SVC representations adopted in [17], [18], [19], [20], and [21] can hardly be considered in real-world applications since the SVC reactive power in these models is optimized in a centralized fashion to enhance the system's performance, while in reality, the SVC responds to limited available voltage measurements. Models presented in [15], [16], and [22] impose that the voltage magnitude at the SVC connection point must remain constant regardless of the occurrence of a contingency. Although such an approach can be implemented in real-world applications, it is very conservative and either results in the insertion of very large SVCs or ultimately leads to the avoidance of SVC allocation. The model adopted in this paper features a droop characteristic in the Q/V relationship, which reflects the actual operation of an SVC and is less restrictive than maintaining a constant voltage at the connection point. In line with existing formulations, both voltage magnitude and stability margin are enhanced considering normal and contingency operations. However, important real-world characteristics regarding the operation of SVCs are integrated into the optimization model. Among them, it should be highlighted: modeling the Q/V operating curve, setting the reference voltage of the controlled bus, and considering the possibility of remote voltage control (this hypothesis assumes the existence of a communication system). The consideration of this more accurate representation significantly increases the problem's search space in comparison with existing approaches. Moreover, the binary nature of the allocation decision variable makes the problem an instance of mixed integer non-linear programming, which is difficult to handle with existing commercial solvers, especially for large instances; thus, we propose a novel metaheuristic-based method specifically designed for this task. The comparison between this proposal and the existing state-of-the-art research for SVC allocation is presented in Table 1. In this sense, the main contributions presented in this paper are as follows:

1) Proposal of an SVC allocation model considering a more accurate model of the SVC than the existing in the literature [15], [16], [17], [18], [19], [20], [21], [22];

TABLE 1. Comparison between this proposal and the state-of-the-art.

Ref.	Optimal sizing	VSI	SVC model	Minimizes number of devices	RCB	VSM	Contingency scenarios	Objective Function	Solution technique
[1]	✓	✗	Variable suscep-tance	✗	✗	✓	✗	Minimize losses and allocation cost	WOA
[9]	✗	✗	Not detailed	✗	✗	✓	✗	Minimize losses and maximize stability margin	ABC
[10]	✓	✓	Firing angle model	✗	✗	✓	✗	Maximize voltage security margin	GA
[11]	✓	✓	Variable reactive power	✗	✗	✗	✗	Maximize system loadability without voltage and power flow violation	GA
[12]	✓	✗	Variable Suscep-tance	✓	✗	✓	✗	Maximizes loading factor and minimizes reactive compensation	MILP
[13]	✓	✓	Variable Suscep-tance	✓	✗	✗	✗	Minimizes losses and voltage deviation	SOCP
[14]	✓	✗	Variable reactive power	✗	✗	✗	✗	Minimize losses	SOCP
[16]	✓	✗	Variable reactive power	✗	✗	✗	✓	Minimize operational cost	Sensitivity based
[17]	✓	✗	Variable Suscep-tance	✓	✗	✓	Most severe only	Minimize operational cost including voltage collapse	Benders decompo-sition
[18]	✓	✗	Variable Suscep-tance	✓	✗	✓	✓	Maximize system voltage stability margin	Bender decompo-sition
[21]	✓	✗	Variable reactive power	✓	✗	✓	✗	Minimize investment and operating costs and maximize VSM	GA
[22]	✓	✗	Variable Suscep-tance	✓	✗	✗	✓	Minimize allocation cost	MINLP
This Proposal	✓	✓	Q/V droop curve	✓	✓	✓	✓	Minimize voltage severity and penalize voltage stability margin	VNS

Note: VSI - Voltage Severity Index; RCB - Remote Controlled Bus; VSM - Voltage Stability Margin; TCSC - Thyristor Controlled Series Capacitor; UPFC - Unified Power Flow Controller; TCVR - Thyristor Controlled Voltage Regulator; TCPST - Thyristor Controlled Phase Shifting Transformer; WOA - Whale Optimization Algorithm; ABC - Artifical Bee Colony; GA - Genetic Algorithm; SPEA - Strength Pareto Evolutionary Algorithm.

2) In addition to the SVC sizing, commonly addressed in the existing literature, the proposed model also considers the optimization of the slope of the Q/V curve and the specified reference voltage of the controlled bus, which is not featured in other research;
3) Inclusion of the possibility of remote voltage control in the optimization model, assuming the existence of communication infrastructure;
4) Maximization of the system's loadability considering a preventive operation mode, i.e., voltage setpoints and the state of discrete shunt elements are kept constant for every operational condition (normal or contingency);
5) Proposing a Variable Neighborhood Search (VNS)-based algorithm tailored to solve the mixed-integer nonlinear optimization problem of SVC allocation and sizing under different system conditions since off-the-shelf solvers are not able to solve the problem.

In addition to this Introduction section, this article is structured as follows. The SVC operational characteristics as well as the optimization problem development are presented in Section II. Numeric results are divided into two sections. Section III describes the metaheuristic developed to tackle the optimization problem addressed in this paper. Numeric results obtained using the proposed metaheuristic to solve

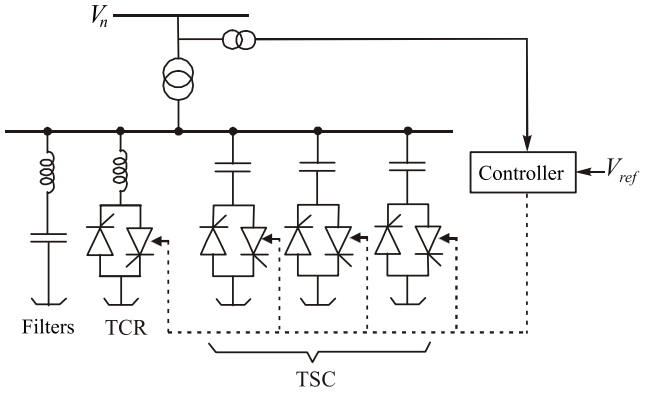

FIGURE 1. Simplified SVC diagram.

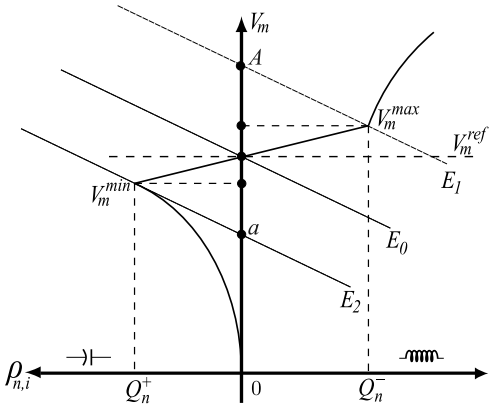

FIGURE 2. Q/V operating curve of the SVC.

the optimization problem developed in this paper is exposed in Section IV. Finally, relevant conclusions are drawn in Section V.

II. PROBLEM FORMULATION

This section presents the main aspects of SVC, the system's operational performance indices, and the definition of the proposed optimization problem.

A. STATIC VAR COMPENSATOR

The SVC is a shunt-connected FACTS device composed of Thyristor-Switched Capacitor (TSC) and Thyristor-Controlled Reator (TCR), as illustrated in Figure 1. The combination of these components allows for continuous modulation of reactive power within its inductive and capacitive limits. Reactive power compensation is achieved by switching the capacitor banks of the TSC and by continuously regulating the inductance of the TCR between their minimum and maximum values [6].

In steady-state studies, the SVC is represented as a controlled shunt element that combines a capacitor bank and reactor behavior. Consider an SVC installed at bus n, with inductive and capacitive susceptance $B_n^{ind} = \frac{Q_n^-}{(V_n^{nom})^2}$ and $B_n^{cap} = \frac{Q_n^+}{(V_n^{nom})^2}$, respectively (where V_n^{nom} is the nominal voltage of the SVC), that controls the voltage at the remote bus m by varying its reactive power output ϱ_n. The reactive power output of this device can be divided into three operating regions: linear, capacitive, and inductive [23], as illustrated in Figure 2. Thus, the reactive power injected/absorbed by the SVC (ϱ_n) may be mathematically formulated as shown in (1).

$$\varrho_n = \begin{cases} B_n^{cap} \cdot V_n^2 & \text{if } V_m \le V_m^{min} \\ \dfrac{V_m - V_m^{ref}}{s_n} & \text{if } V_m^{min} < V_m < V_m^{max} \\ B_n^{ind} \cdot V_n^2 & \text{if } V_m \ge V_m^{max} \end{cases} \quad (1)$$

where V_n represents the voltage magnitude at the allocation bus n of the SVC. V_m^{ref} represents the the reference voltage magnitude for the controlled bus m. Note that, when the voltage of the controlled bus is between V_m^{min} and V_m^{max}, the reactive power is described by a linear characteristic, defined as the difference between the controlled bus voltage and the reference voltage, divided by the slope of the SVC's operating curve (s_n). However, when the voltage of the controlled bus falls below V_m^{min} or exceeds V_m^{max}, the behavior of the SVC is governed by the passive response of the shunt reactance to the nodal voltage, giving rise to the nonlinear behavior depicted in Figure 2.

In Figure 2, line E_0 (and those parallel to it) represents the voltage that would be observed at bus m considering different operating conditions. E_0 represents an operating condition where no reactive power compensation is required, and thus the controlled bus voltage is equal to the reference voltage ($V_m = V_m^{ref}$). Under more stressed system conditions, such as those indicated by E_1 (overvoltage system condition) and E_2 (undervoltage system condition), the voltage at the controlled bus would shift to points A and a, respectively, in the absence of SVC control. However, with proper SVC operation, the voltage is regulated back to within acceptable limits specifically, from A to $V_m^{\max}$ and from a to $V_m^{\min}$ [24].

B. VOLTAGE SEVERITY INDEX - STEADY-STATE VOLTAGE MAGNITUDE ANALYSIS

In the proposed approach, the SVC installation must mitigate voltage magnitude violations under all analyzed operating conditions, i.e., during both normal and contingency scenarios. To this end, voltage magnitude violation is calculated for all buses in the EPS for each scenario, as defined in (2). These violations are then aggregated and converted into a Voltage Severity Index (VSI), which quantifies the system-wide accumulated voltage violation severity across all operating scenarios, as defined in (2) and (3).

$$VV_{n,i} = \max\{0; V_{n,i} - \overline{V}_n; \underline{V}_n - V_{n,i}\} \quad (2)$$

$$VSI = \sum_{i \in \Omega_C} \sum_{n \in \Omega} \left(VV_{n,i}^2\right) \quad \forall i \in \Omega_C, \forall n \in \Omega \quad (3)$$

where Ω_C is the set of operating scenarios, Ω is the set of system buses, $\overline{V}_n$ and $\underline{V}_n$ are the upper and lower operational limits for the voltage magnitude at bus n, $V_{n,i}$ is the voltage

magnitude calculated for bus n in the operating scenario i, and $VV_{n,i}$ is the magnitude of the voltage violation at bus n under scenario i.

C. VOLTAGE SECURITY MARGIN - VOLTAGE STABILITY ANALYSIS

The system stability is defined in [24] as the ability of the EPS, given an initial operating condition, to reach a new state of equilibrium after a physical (small or large) disturbance, while maintaining its electrical variables within acceptable limits and the system as a whole largely intact. Hence, with a specific focus on voltage, it can be stated that voltage stability refers to the ability of an EPS to maintain acceptable voltage levels in all buses following disturbances. In contrast, voltage collapse is a process in which a sequence of events, initiated by voltage instability, leads to abnormally low voltage levels across significant regions of the system [25].

Mathematically, voltage collapse corresponds to a *Saddle-Node* bifurcation point in the power flow equations, characterized by the Jacobian matrix becoming singular, signaling a loss of feasible solutions [26]. In practical terms, this bifurcation occurs when two power flow solutions (one stable and one unstable) converge and disappear as system parameters, typically the system's load, gradually increase [25]. Given that reaching the voltage collapse point can lead to severe problems for EPS operators, it is crucial that they understand how far the system is operating from this critical condition. This distance is referred to as the VSM or margin to instability. In the specific literature, it is possible to find several methods to evaluate this distance, with one of the most commonly used being the loading margin. Taking into account a specific operating point, the loading margin is defined as the maximum additional load that the system can accommodate before achieving the collapse point [27]. It is important to highlight that the loading margin is influenced by the direction of the increase in system load, as well as by the power re-dispatch from the generators.

The VSM can be computed using the CPF method proposed in [28]. Although the VSM can be determined and used in the optimization model, a major concern in this work is identifying secure operating points for the EPS. Although VSM focuses on the ability of the system to maintain stability under various conditions, the voltage security margin emphasizes the safety buffer between actual voltage levels and predefined voltage limits. Both margins are crucial for ensuring the robustness and reliability of power systems. Both the voltage security margin and VSM are illustrated in Figure 3.

In this approach, the VSM is integrated into the objective function as a penalization factor, which is calculated as per (4).

$$VSM = \kappa^{\mu} \sum_{i \in \Omega_C} \max\{0; \underline{\mu} - \mu_i\} \tag{4}$$

where $\underline{\mu}$ is the minimum acceptable stability margin for the system and μ_i is the stability margin calculated for scenario i.

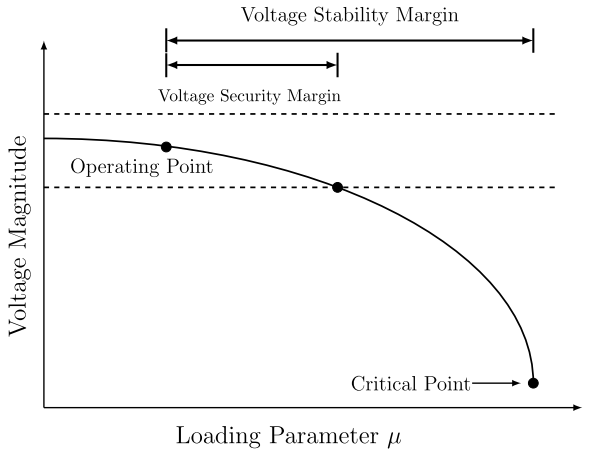

FIGURE 3. Illustration of voltage security and stability margins.

The value μ defines the point at which the system operates in the region considered safe in terms of voltage stability, as illustrated in Figure 3.

By aggregating VSI and VSM analyzes into the optimization problem, voltage violations can be effectively mitigated or eliminated, while simultaneously enhancing the system's robustness to gradual load increases.

It should be highlighted that the results presented in this paper were obtained considering the constant power model for the loads. This model yields conservative results compared to the other load models, under which voltage-dependent components reduce power demand as the voltage decreases, thus extending stability margins. For systems dominated by fast-response loads (e.g. motor-dominated loads), detailed dynamic modeling is essential to capture specific instabilities, as conventional power flow models an PV curves may be insufficient [29].

D. OPTIMIZATION MODEL

An optimization problem that incorporates the EPS operation as a constraint and includes binary decision variables (such as SVC allocation) can be formulated as the Mixed Integer Nonlinear Programming (MINLP) problem:

$$min \;\; F(\mathrm{X}) \tag{5}$$

$$\text{s.t. } g_i(\mathrm{X}) = 0 \quad i = 1, \ldots, k \tag{6}$$

$$h_i(\mathrm{X}) \leq 0 \quad i = 1, \ldots, m \tag{7}$$

$$\mathrm{X} = [x_1, x_2, \ldots, x_p] \tag{8}$$

$F(x)$ is the objective function to be minimized, X represents the vector of decision variables x, $g(X)$ represents the set of equality constraints, $h(X)$ represents the set of inequality constraints, and k, m, and p are the number of equality, inequality constraints, and decision variables, respectively.

The goal of the formulation proposed in this paper is to determine the best allocation and size of SVCs to minimize voltage violations and maximize system robustness (i.e., increase the voltage stability margin). Since the installation of SVCs involves capital investment, it is desirable to allocate

the minimum capacity necessary to ensure operational security. Additionally, certain operating scenarios may exhibit numerical ill-conditioning, which prevents the solution of the power flow equations. In such cases, it is not possible to calculate the VSI or the VSM. Although non-convergence does not necessarily indicate a critical operating condition, it is also it also does not guarantee the operational security of the scenario. Therefore, it is essential to account for the number of non-convergent scenarios for each SVC allocation solution. Considering all these aspects, the objective function proposed in (9) is adopted for the optimization problem.

$$\min\ \kappa^{v}\sum_{i\in\Omega_C}\sum_{n\in\Omega}\left(VV_{n,i}^{2}\right)+\kappa^{s}\sum_{n\in\Omega}\left(Q_n^{-}+Q_n^{+}\right)+\kappa^{nc}\sum_{i\in\Omega_C}\alpha_i+\kappa^{\mu}\sum_{i\in\Omega_C}\max\{0;\underline{\mu}-\mu_i\} \tag{9}$$

The first term corresponds to the minimization of the VSI, calculated according to (3). The second term represents the acquisition cost of the SVC, modeled as a linear function of its reactive power rated capacity. The third term penalizes non-convergent scenarios, with the binary variable $\alpha_i = 0$ indicating that the operating point i is convergent and $\alpha_i = 1$ indicating a non-convergent condition. Finally, the fourth term penalizes scenarios in which the VSM (μ_i) falls below a predefined threshold $\underline{\mu}$. The inclusion of the VSM in the objective function reflects the intention to favor SVC allocation solutions that operate in a secure region. However, unlike imposing stability margin limits as constraints, this approach does not discard solutions that fail to meet this criterion, which could otherwise lead to an empty set of solutions.

The operation of the SVC within an EPS is subject to operational constraints and system limitations which can be described using the power flow equations. Accordingly, the feasible solution space of the proposed optimization model is bounded by a set of technical constraints, as shown in (10)–(18).

Constraints given by (1), (2), and (3) (10)

$$\underline{s} \le s_n \le \overline{s} \tag{11}$$

$$0 \le Q_n^{-} \le \overline{Q}x_n \tag{12}$$

$$0 \le Q_n^{+} \le \overline{Q}x_n \tag{13}$$

$$\underline{V}_n \le V_m^{ref} \le \overline{V}_n \tag{14}$$

$$\sum_{n\in\Omega} x_n \le \overline{N}^{svc} \tag{15}$$

$$P_{n,i} - V_{n,i}\sum_{m\in\Omega_n} V_{m,i}(G_{n,m}cos\theta_{n,m,i} + B_{n,m}sen\theta_{n,m,i}) = 0 \tag{16}$$

$$Q_{n,i} - V_{n,i}\sum_{m\in\Omega_n} V_{m,i}(G_{n,m}\sin\theta_{n,m,i} - B_{n,m}\cos\theta_{n,m,i}) + \varrho_{n,i} = 0 \tag{17}$$

$$x_n, \alpha_i \in \{0,1\} \quad \forall n \in \Omega, \forall nm \in \Omega_L, \forall i \in \Omega_C \tag{18}$$

Note that the SVC Q/V curve, defined by (1), depends on the slope s_n and the inductive and capacitive capacities, which are constrained by (11), (12), and (13), respectively. The installed capacity of the SVCs is limited by the maximum nominal value $\overline{Q}$ and is modulated by the binary variable x_n, which indicates the presence ($x_n = 1$) or absence ($x_n = 0$) of an SVC at bus n. Constraints (2) and (3) (included in (10)) are necessary to calculate the VSI, used in the objective function. Constraint (15) sets an upper limit $\overline{N}^{svc}$ on the number of SVCs available for installation in the EPS. Equations (16) and (17) represent the active and reactive power balance, incorporating the contribution of the SVC ($\varrho_{n,i}$) in the reactive power balance; taking into account voltage magnitudes, the angular difference between two buses ($\theta_{n,m,i}$), the net active and reactive power consumptions ($P_{n,i}$ and $Q_{n,i}$), and the system's admittance matrix ($Y_{n,m} = G_{n,m} + jB_{n,m}$). Lastly, constraint (18) defines the binary nature of variables x_n and α_i.

III. PROPOSED METHODOLOGY

Solving MINLP problems, such as the one proposed in this work, is not an easy task, even when simplifications are considered. Due to the non-convex characteristics of the problem and its multimodal nature, attaining a solution using commercial solvers may require a long time, and in most cases, it is not possible to guarantee its optimality. This complexity is further amplified by the simultaneous need to optimize both the location and the operational parameters of the SVCs, including the slope of the Q/V curve, reactive power limits, controlled bus, and reference voltage. The strong interdependencies among these decision variables, coupled with the nonlinearities of the power flow equations, render the problem combinatorially complex. For instance, once a promising location for an SVC is identified, adjusting its operational parameters may alter its effectiveness or reveal more advantageous alternatives, which demands optimization techniques capable of balancing global exploration with local exploitation.

As reported in several fields that make use of optimization techniques, metaheuristics can efficiently solve this type of problem without the need for simplifications and demanding less computational time [30]. In this work, the VNS algorithm was adopted, given its suitability for problems characterized by multiple local optima and strong coupling among variables. By systematically alternating between different neighborhood structures, the VNS increases the chances of escaping local optima and identifying competitive solutions in complex search spaces. This capability is particularly advantageous for the problem at hand, where diverse combinations of location, capacity, and operational settings of SVCs, typically attained in population-based metaheuristic, may lead to multiple suboptimal configurations.

In order to manage both computational complexity and technical feasibility, a combined strategy integrating the VNS algorithm and the commercial power flow software ANAREDE® [31], widely used by the Brazilian TSO, was adopted.

The VNS algorithm determines the placement and parameters (namely, capacity, slope of the Q/V curve, location, controlled bus, and voltage magnitude reference) of the SVCs (i.e., decision variables), while ANAREDE® evaluates the corresponding operating condition (ensuring the equality constraints of the problem) and allowing the technical feasibility assessment of each solution (inequality constraints). This approach leverages the VNS's ability to efficiently explore the solution space, along with the accuracy and efficiency of a commercial software for solving power flow equations, thus enabling an effective and reliable solution methodology for the proposed optimization problem.

The VNS is a local search-based metaheuristic that systematically varies the neighborhood structures during the search process to escape local optima and explore the solution space more thoroughly [32]. Originally introduced in [33], the VNS has demonstrated to be effective in representing and solving a wide range of operational research problems, including combinatorial and nonlinear optimization. The algorithm starts with a randomly generated solution to which perturbations, defined by predefined neighborhood structures, are applied to obtain neighboring solutions. If a neighboring solution improves the objective function, it becomes the new current solution; otherwise, the algorithm modifies the concept of neighborhood to generate new neighboring solutions, thereby exploring a broader region of the search space.

Evidently, the ability of the VNS algorithm to achieve high-quality solutions depends on how well it can explore the search space. In turn, an efficient exploration process depends on 1) how the solutions are encoded, 2) the neighboring solutions are determined and 3) the neighborhood structures are defined. In this sense, the remainder of this section is devoted to addressing these concepts.

A. SOLUTION ENCODING

The effectiveness of the VNS algorithm relies on the quality of solution encoding, which must adequately capture the variables involved in the location and sizing of SVCs. We propose encoding each solution using the matrix $\hat{X}$, as illustrated in (19). This matrix incorporates the decision variables for each potential SVC (up to $\overline{N}^{svc}$), namely: the allocation bus (n), the controlled bus (m), the Q/V curve slope (s_n), the inductive (Q_n^-) and capacitive (Q_n^+) capacities, and the reference voltage (V_m^{ref}). This structure enables the VNS to efficiently explore the search space while accounting for the interdependencies among the operational parameters of the SVC.

$$\hat{X} = \begin{bmatrix} x_1 & n_1 & m_1 & s_1 & Q_1^- & Q_1^+ & V_{m_1}^{ref} \\ x_2 & n_2 & m_2 & s_2 & Q_2^- & Q_2^+ & V_{m_2}^{ref} \\ \vdots & \vdots & \vdots & \vdots & \vdots & \vdots & \vdots \\ x_r & n_r & m_r & s_r & Q_r^- & Q_r^+ & V_{m_r}^{ref} \end{bmatrix}, \quad r = \overline{N}^{svc} \tag{19}$$

It is important to note that the allocation and controlled voltage buses do not necessarily coincide. The voltage control strategy considering remote buses, although possible, involves additional costs related to communication infrastructure and advanced control techniques, and may not be feasible in certain network configurations. To reflect these practical limitations and reduce computational complexity, the set of candidate controlled buses is restricted to those adjacent to the SVC location, as well as buses directly connected to them. Consequently, the set of possible controlled buses m is dependent on the allocation bus n.

B. NEIGHBORHOOD STRUCTURES

The VNS algorithm begins from an initial solution and generates a set of neighboring solutions, each of which is evaluated based on the objective function. If a neighboring solution presents a better objective function value than the current solution, it becomes the new current solution. However, if no improvement is identified, the algorithm employs a different, broader neighborhood structure, progressively expanding the search scope to explore additional possibilities. Clearly, there must be a finite number of neighborhood structures and none of them can encompass the entire search space, otherwise the VNS would simply become an exhaustive search algorithm. In this work, we propose the five neighborhood structures. Each structure performs different modifications in the current solution to create neighboring solutions. The alterations made by each neighboring structure to the current solution are detailed bellow:

1) The first neighborhood structure simultaneously alters the SVC allocation bus (from n to n') and the controlled bus (from m to m'), considering the set of remotely controllable candidate buses for each n'. The new allocation bus n' is randomly chosen from buses adjacent to the current position n and a subset of buses distributed across the EPS. Then, the controlled bus m' is randomly selected from the set of candidate buses associated with the new allocation bus n'.
2) The second neighborhood structure modifies only the controlled bus (from m to m'), keeping the allocation bus (n) fixed. The controlled bus m' is randomly chosen from the set of candidate buses defined for the current allocation bus n.
3) The third neighborhood structure alters the SVC reactive capacities (from Q^- and Q^+ to $Q^{-'}$ and $Q^{+'}$), generating new random values within the limits specified by (12) and (13). This structure also allows setting the capacity of some SVCs to zero, enabling the exploration of configurations with fewer devices.
4) The fourth neighborhood structure adjusts the SVC Q/V operating slope (from s_n to s'_n), selecting random continuous values within the bounds defined by (11).
5) The fifth neighborhood structure modifies the reference voltage (from V_m^{ref} to $V_m^{ref'}$) at the controlled bus, randomly adjusting the value within the limits defined in (14).

The number of SVCs modified in each neighborhood structure is determined randomly, introducing variability in the perturbations. An iteration is completed when all neighborhood structures have been explored and the current solution remains unchanged. The search terminates when a predefined number of iterations is reached.

C. VNS ALGORITHM PSEUDOCODE

The pseudocode of the proposed VNS algorithm, presented in Algorithm 1, outlines the optimization process for the allocation and sizing of SVCs in EPSs. The algorithm begins with an initial randomly generated solution $\hat{X}_0$, which serves as the starting point for the search. The current solution $\hat{X}$ is iteratively updated based on the evaluation of the objective function $f(\hat{X})$, responsible for quantifying the performance of the solution $\hat{X}$. The process uses k_{max} neighborhood structures and is constrained by a maximum number of iterations, it_{max}.

In each iteration, the algorithm generates a set of neighboring solutions N^k using the function $N^k(\hat{X}, j)$, which randomly modifies the parameters of j SVCs, with j varying between 1 and $\overline{N}^{svc}$. For each neighborhood structure k, P^k neighboring solutions are generated, and the best neighbor $\hat{X}'$ is identified. If $\hat{X}'$ yields a better objective function value than the current solution, $\hat{X}$ is updated to $\hat{X}'$, and the search returns to the first neighborhood ($k \leftarrow 1$); otherwise, the algorithm proceeds to the next neighborhood structure ($k \leftarrow k+1$). This process combines randomness and systematic exploration, enabling VNS to escape local optima and converge to high-quality solutions.

Algorithm 1 Pseudocode of the Proposed VNS Algorithm

Require: $\hat{X}_0, k_{max}, it_{max}, f(\hat{X}_0), P^k$
  $\hat{X} \leftarrow \hat{X}_0$
  $f(\hat{X}) \leftarrow f(\hat{X}_0)$
  for $i = 1$ **to** it_{max} **do**
    $k \leftarrow 1$
    while $k \leq k_{max}$ **do**
      for $p = 1$**to**P^k **do**
        $j = Random\_Number(1, \overline{N}^{svc})$
        $N_p = \mathcal{N}^k(\hat{X}, j)$
      end for
      $N^k \leftarrow N_p$
      $\hat{X}' \leftarrow \min\{f(\hat{Y}) | \hat{Y} \in N^k\}$
      if $f(\hat{X}') < f(\hat{X})$ **then**
        $\hat{X} \leftarrow \hat{X}'$
        $k \leftarrow 1$
      else
        $k \leftarrow k + 1$
      end if
    end while
  end for
  return $\hat{X}$

IV. TEST AND RESULTS

The effectiveness of the developed algorithm was verified using the IEEE 57 bus system and a simplified 107-bus version of BIPS [34]. For these systems, we considered the possibility of installing up to three SVCs ($\overline{N}^{svc} = 3$). To ensure an adequate SVC operational response, a range of 1%–5% Q/V slope was adopted for the SVCs [35]. The maximum reactive power capacity ($\overline{Q}$) was set at 80 MVAr, while the minimum VSM (μ), which defines the voltage security region, was fixed at 4%, according to the Brazilian TSO guidelines [36]. The penalty parameters were set as follows: $\kappa^v = 10000$, $\kappa^s = 1$, $\kappa^{nc} = 100$, and $\kappa^{\mu} = 1000$. A predefined set of $N-1$ contingencies in each system was considered to evaluate both the VSI and VSM.

The VSM for each scenario was determined using the CPF method, applying a 10% of initial load step increase in all areas of the system, maintaining their power factors constant. This increase in load demand requires the redispatch of the generation units to meet the additional demand. The redispatch was calculated using a participation factor (PF_k), based on generation under normal operating conditions (i.e., without contingencies or load increase), as defined in (20).

$$PF_k = \frac{P_k^g}{\sum_{k \in \Omega_g} P_k^g} \tag{20}$$

where P_k^g is the active power generated by unit k, and Ω_g is the set of all generation units.

The VNS algorithm was implemented in Python, and the power flow calculations required to evaluate the system performance under normal and contingency conditions (power flow and CPF), were performed using the ANAREDE® software. [31]. All simulations were executed on a personal computer equipped with an Intel® Core™ i7-10700 processor running at 2.90 GHz and 32 GB of RAM.

A. IEEE 57-BUS SYSTEM

The IEEE 57-bus system is a well-established benchmark for power system optimization studies, representing a medium-scale transmission network derived from a segment of the American Electric Power (AEP). This system consists of 57 buses, including 7 generator buses, with the remaining 50 PQ (load) buses serving as candidates for SVC allocation. The network includes 80 transmission lines and 17 transformers, with no SVCs in the base configuration, and supports a total demand of 1250.8 MW and 336.4 MVAr. Voltage magnitudes are constrained to 0.95–1.05 p.u. Of the 80 N-1 contingencies analyzed, corresponding to the 80 transmission lines, one was non-convergent in the original configuration. The best SVC configuration obtained by the VNS algorithm is presented in Table 2, with performance improvements over the base case summarized in Table 3.

The algorithm strategically selected buses 34, 33, and 52 for SVC installation, utilizing capacities of ±15 MVAr, ±11 MVAr, and ±51 MVAr, respectively, despite the availability of up to 80 MVAr. This efficient allocation, with carefully tuned slopes and reference voltages, ensured operation within safe voltage limits (0.95–1.05 p.u.) and

TABLE 2. SVC best operational characteristics for IEEE 57 bus system.

	Allocation Bus	Controlled bus	Slope (%)	Capacity (MVAr)	Reference voltage (p.u.)
SVC 1	34	33	1.29	± 15	1.047
SVC 2	33	32	3.55	± 11	1.049
SVC 3	52	52	1.29	± 51	1.049

TABLE 3. Results for the IEEE 57-bus system.

	Original system	VNS best solution
VSI	19,434.3	347.5
Lower VSM	2.81 %	14.68 %
Non-convergent cases	1	0
Objective Function	21698.7	424.5

minimized the impact of critical contingencies, demonstrating the algorithm's ability to prioritize effective reactive power support over excessive capacity.

As shown in Table 3, the VNS solution significantly improved key performance metrics compared to the original system configuration. The VSI dropped from 19,434.3 to 347.5, a 98.21% reduction, reflecting a near-elimination of voltage violations across all considered contingencies. The lowest VSM increased from 2.81% to 14.68%, indicating enhanced system robustness against voltage collapse. The objective function value improved by 98.04%, from 21698.7 to 424.5. These outcomes highlight the VNS algorithm's effectiveness in identifying optimal SVC placements to achieve secure and stable operation under normal and critical contingency conditions.

B. 107-BUS TEST SYSTEM

A more detailed analysis was conducted on the 107-bus test system, a simplified representation of the BIPS, to evaluate the effectiveness of the VNS algorithm. The system comprises 107 buses, including 83 PQ (load) buses designated as candidates for additional SVC installation, with one SVC already present in the base configuration. A total of 135 $N-1$ contingencies were considered as operating scenarios in addition to the normal operating scenario. It is worth noting that, considering the system's original configuration (without additional SVCs installation), 16 out of the 136 operating scenarios (i.e., the normal operation and the 135 contingencies) did not converge. The test system is illustrated in Figure 4, since it is less well-known than the 57-bus system, and further details about its data can be found in [37].

1) DEFINITION OF THE CASE STUDIES

The quality of solutions found by the algorithm was validated considering three case studies:

- **Base Case**: Original configuration used as a reference case. This system includes a single SVC at bus 4530.
- **Case A**: The best solution obtained by the VNS algorithm when the VSM penalty is disregarded ($\kappa^{\mu} = 0$). This represents a simplified version of the developed algorithm, focused solely on minimizing voltage violations under normal and contingency conditions.

TABLE 4. SVC operational characteristics for the original configuration of the 107-bus system (Base Case).

	Allocation Bus	Controlled bus	Slope (%)	Capacity (MVAr)	Reference voltage (p.u.)
SVC 1	4530	4530	0.01	± 64	1.020

TABLE 5. SVC operational characteristics for Case A.

	Allocation Bus	Controlled bus	Slope (%)	Capacity (MVAr)	Reference voltage (p.u.)
SVC 1	4522	4501	1.24	± 64	1.045
SVC 2	138	120	2.28	± 70	1.033
SVC 3	4530	4533	3.69	± 26	1.012

TABLE 6. SVC operational characteristics for Case B.

	Allocation bus	Controlled bus	Slope (%)	Capacity (MVAr)	Reference voltage (p.u.)
SVC 1	106	106	4.91	± 77	1.036
SVC 2	4501	4532	3.76	± 66	1.043
SVC 3	140	140	1.04	± 67	1.040

- **Case B**: The best solution obtained by the VNS algorithm with the the VSM penalty included ($\kappa^{\mu} = 1000$). This version considers both the maximization of the voltage stability margin and the minimization of voltage violations under normal and contingency conditions.

Cases A and B are solved assuming there is no SVC at bus 4530. It should be noted that, in Case A, the objective function does not penalize VSMs values below the threshold 4%, focusing exclusively on minimizing voltage violations and the associated costs of SVCs installation. In contrast, Case B introduces a penalty for solutions exhibiting VSM values below 4%, thereby encouraging more robust solutions. The operational characteristics of the SVCs obtained for the three case studies are presented in Tables 4, 5, and 6. It should be noted that the solutions obtained in Cases A and B reduce the number of non-convergent contingencies from 16 (in the Base Case) to 15, as a result of the additional SVCs installed.

2) VOLTAGE SEVERITY INDEX ANALYSIS

A comparison of the system's performance in terms of voltage violations for the three case studies is presented in Table 7. For the sake of conciseness, only the five most critical contingencies are shown. Note that: 1) the two most critical contingencies account for more than half of the total VSI of the system (84%, 64%, and 82% for the Base, A, and B cases, respectively), and 2) cases A and B reduce the total VSI by 61% and 54%, respectively, compared to the Base Case, primarily by mitigating the impact of these two contingencies.

Figures 5 and 6 present boxplots of the nodal voltage magnitudes computed for all convergent operating scenarios, considering the SVCs allocations of the Base Case and Case B, respectively. The boxplot of the voltages obtained for Case A is omitted due to its similarity to Case B.

In Figure 5, overvoltage events exceeding 1.15 p.u. and undervoltages below 0.90 p.u. can be observed, underscoring

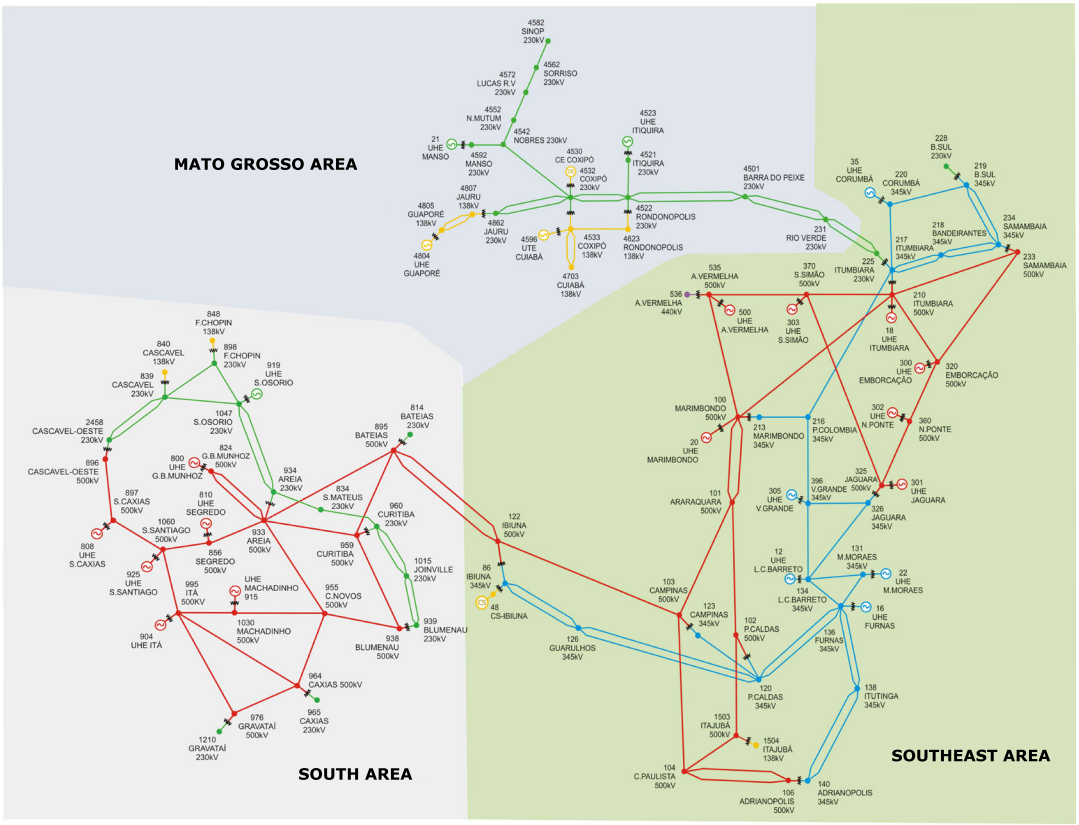

FIGURE 4. One-line diagram of the simplified 107-bus Brazilian Interconnected Power System, adapted from [34].

TABLE 7. Comparison of voltage severity indices.

Line under contingency	VSI associated with the contingency		
	Base Case	Case A	Case B
104 - 1503	234.2	23.4	0.0
4862 - 4807	125.8	84.5	142.2
934 - 933	19.2	19.3	19.1
103 - 123	17.8	10.6	14.9
233 - 320	14.5	12.6	14.2
Total VSI	428.5	166.8	196.2

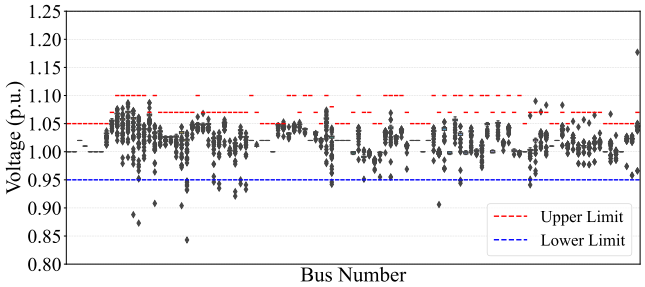

FIGURE 5. Nodal voltage for each contingency event - Base Case.

vulnerabilities in the original system configuration. In contrast, Figure 6 illustrates that, in Case B, although voltage violations are not entirely eliminated, voltage dispersion is significantly reduced, with fewer extreme values. This reflects a significant mitigation of voltage violation severity due to contingency events, confirming the robustness of the optimized solution.

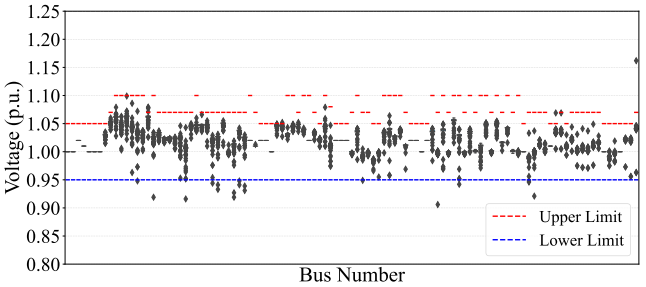

FIGURE 6. Nodal voltage for each contingency event - Case B.

3) VOLTAGE STABILITY MARGIN ANALYSIS

The VSM indicates the operational distance of the system from the voltage collapse point for each operational scenario i, making it a key indicator for evaluating system robustness against load increases. To emphasize the effective loading margins in the analyzed operating scenarios, the convergent contingencies were ranked based on their margin values. The five most critical contingencies for each case study are presented in Table 8.

For the Base Case, two of the five most critical contingencies (104-1503 and 225-231) exhibit VSM below the 4% threshold, with the contingency of line 104-1503 being particularly severe (0.625%). This indicates a critical proximity between the operating point and the voltage collapse, highlighting the vulnerability of the original system to load increases in this scenario.

TABLE 8. Voltage stability margin of the most critical contingencies.

Base Case		Case A		Case B	
LUC	VSM	LUC	VSM	LUC	VSM
104 - 1503	0.625	4501 - 4522*	1.249	104 - 1503	4.00
225 - 231	3.000	104 - 1503	1.999	4501 - 4522*	4.687
102 - 1503	4.687	995 - 1060	4.875	995 - 1060	5.125
1030 - 955	5.375	1030 - 955	5.625	1030 - 955	6.812
101 - 102	5.938	959 - 895	6.749	959 - 895	7.245

LUC - line under contingency
* The contingency of line 4501 - 4522 is non-convergent in the original configuration (Base Case)

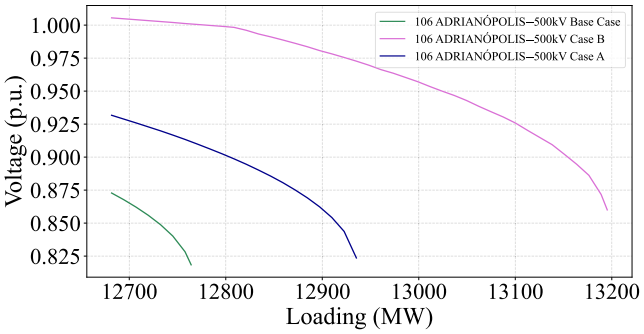

FIGURE 7. PV curve of the critical bus considering the loss of line 104-1503.

In Case A, two contingencies still show a VSM below 4%; however, the margin associated with the contingency related to the line 104-1503 increases significantly. Notably, the 225-231 line contingency, which violated the VSM threshold in the Base Case, is no longer among the most critical in Case A and does not breach the 4% limit. Additionally, contingency 4501-4522, which was non-convergent in the Base Case, becomes convergent in Case A.

Case B, in turn, not longer presents a contingency with a VSM below the 4% threshold. It is important to note that the worst VSM is observed for contingency 104-153 which falls at the minimum permitted limit of 4%. This value represents a 540% increase compared to the Base Case and an 100.1% improvement compared to Case A. The VSM enhancement is not an inherent characteristic of the VNS algorithm, but rather the result of considering $\kappa^{\mu} > 0$. In this sense, the allocation and sizing of SVCs under the optimization model adopted in Case B yield good-quality solutions only if the most critical VSM is at least 4%, representing a 540% increase relative to the original 0.625%. Moreover, contingency 4501-4522, which violated the VSM threshold in Case A (1.249%), achieves a margin of 4.687% in Case B, thus also exceeding the minimum required threshold.

These results demonstrate that Case B maximizes the VSM compared to both Case A and the Base Case, mainly due to the penalization of VSM violations. Furthermore, as shown in Table 7, the voltage severity indices for Case A (166.8) and Case B (196.2) are similar, indicating that the VSM penalization in Case B not only improves the distance to collapse but also maintains effective mitigation of voltage violations, achieving a balance between both objectives.

The improvement in VSM can be visualized through PV curves, which illustrate the relationship between nodal voltage and load increment, highlighting the distance to the voltage collapse point. For this analysis, we consider the loss of line 104 - 1503, identified as the most critical contingency for the Base Case (since the contingency of line 4501-4522 is non-convergent in this case). Figure 7 illustrates the PV curve for the most critical bus in the system (a 500 kV bus in ADRIANÓPOLIS-PR). Note that the collapse point occurs for a 12,760.96 MW system-wide demand in the Base Case ($\mu = 0.625\%$), increasing to 12,935.33 MW in Case A ($\mu = 1.99\%$) and to 13,189.0 MW in Case B ($\mu = 4.00\%$). Thus, Case B allows for an additional 428 MW loadability compared to the Base Case and 254 MW more than Case A under the most critical line loss event.

In Case B, SVCs are allocated at buses 106 and 140, effectively eliminating the VSI while prioritizing the enhancement of the VSM at bus 106, identified as the collapse bus. Conversely, Case A focuses on mitigating the VSI by placing one SVC near the violated buses in the base case and another at bus 4522 to address the VSI of contingency 135 (the second most critical), which remains unmitigated in Case B. Overall, Case B outperforms Case A by achieving complete VSI resolution and a more substantial VSM improvement at the critical collapse point, thereby ensuring greater system robustness across multiple contingencies.

C. ALGORITHM CONVERGENCE ANALYSIS

As outlined in Section III, the VNS-based methodology employs five neighborhood structures to optimize SVC allocation and sizing. Our experience revealed that the first three neighborhood structures (i.e., adjusting allocation bus (n), controlled bus (m), and SVC reactive power capacities (Q^{-} and Q^{+}) have a significant impact on the objective function due to their combinatorial nature. As for the last two, which modify continuous variables (i.e., Q/V curve slope s_n and reference voltage V_m^{ref}), have a relatively smaller impact due to their constrained ranges. Given the different impacts of each structure on the algorithm's capability of escaping local optima, the number of neighboring solutions to be created for each structure was defined to enhance efficiency, for both test systems, as follows: 20 for the first three structures and 10 for the latter two. In this sense, at least 80 candidate solutions are evaluated per iteration (60 in the three structures that modify integer decision variables and 20 in the two that modify continuous variables). Additionally, it was defined that if the current solution is not replaced after two iterations, the neighborhood exploration order is randomly reconfigured to enhance search diversity.

The algorithm's performance was assessed through 30 independent runs for both test systems, each constrained to a maximum of 40 iterations. For the 57-bus system, the algorithm exhibited consistent convergence, achieving an average objective function value of 436.72 with a standard deviation of 3.28%, and a best solution of 424.5. The

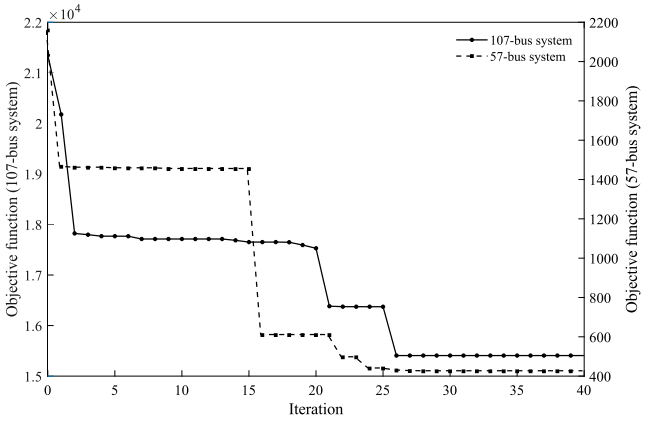

FIGURE 8. VNS Convergence for 107-bus and 57-bus System.

same behavior was observed for the 107-bus system, which achieved the best objective function of 15,399.1, with an average value of 15,959.38 and a standard deviation of 5.14%.

Figure 8 illustrates the evolution of the objective function over iterations for the best solution obtained for each tested system. Both systems converge after approximately 30 iterations, with negligible improvements in the objective function thereafter. The total execution time of 40 iterations was 68,712.91 seconds (19.09 hours) for the 57-bus system and 93,519.49 seconds (25.98 hours) for the 107-bus system. These relatively long runtimes are mainly because each candidate solution requires the execution of power flow analyses under a set of contingencies (80 for the 57-bus system and 135 for the 107-bus system). Moreover, for each contingency, a continuation power flow is performed to estimate the VSM. Consequently, every neighbor generated and evaluated demands considerable computational effort. In addition to the difference in the number of power flow evaluations, the search space size also differs across systems, with 50 candidate buses for SVC placement in the 57-bus system and 83 in the 107-bus system, which is not proportionally reflected in the execution time of the algorithm. It can be observed that the 107-bus system reflects reasonable scalability, as the increase in computational time compared to the 57-bus system is consistent with the larger number of contingencies (from 80 to 135) and candidate buses (from 50 to 83). This demonstrates that the algorithm efficiently handles system complexity, given that the same number of neighbors was used for both systems. Therefore, the execution time could be further reduced by adjusting the number of neighbors according to the system size.

A more detailed convergence analysis for the 107-bus system is presented in Figure 9. The horizontal axis represents the number of solutions explored by the algorithm, while the horizontal lines indicate the end of each iteration. Observe that a total of 6,980 solutions were explored over 40 iterations, with 6,180 (88.53%) evaluated in the first 30 iterations. Since each iteration involves a comprehensive exploration of all neighborhood structures, it is expected that a greater number of intermediate solutions will be identified throughout the exploration process. For instance, the first

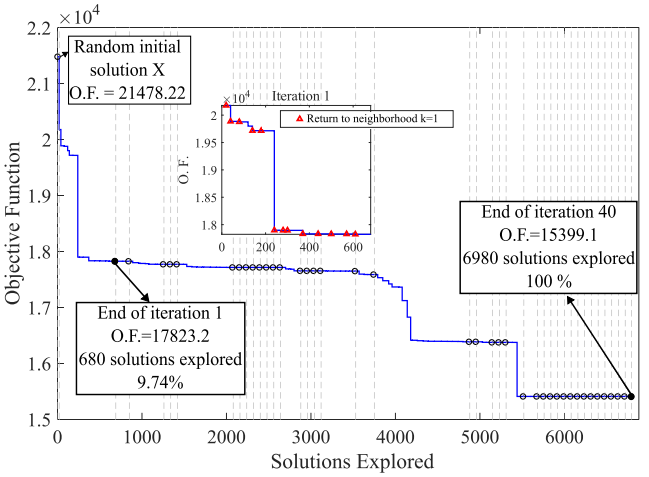

FIGURE 9. VNS detailed convergence for 107-bus system.

iteration started with an initial objective function value of 21,478.22 and, after evaluating 680 candidate solutions, achieved an improved value of 17,823.19 at the beginning of the second iteration. Notably, from iteration 25 onward, a total of 1,470 solutions were explored until the end of iteration 40 without yielding a significant improvement, which provides strong evidence of algorithm convergence.

Attempts to directly solve the optimization problem using off-the-shelf solvers were carried out and failed. The convex power flow formulation proposed in [38] and implemented in the Powermodels.jl package [39] was adopted, along with the objective function presented in [18] (loadability maximization). Then, CPLEX and Gurobi ran for 48h to solve the problem for the 107-bus system and found no feasible solution during that time, thereby reinforcing the importance of the proposed metaheuristic, which can solve an optimization problem that off-the-shelf solvers could not tackle.

V. CONCLUSION

In this work, a Variable Neighborhood Search (VNS) algorithm was developed to address the problem of allocating and sizing SVCs in Electric Power Systems (EPSs), aiming to minimize voltage violations and enhance the Voltage Stability Margin (VSM) under normal and contingency operating conditions. In this regard, SVCs can provide additional reactive support and respond automatically and rapidly to topological changes in the network, such as the N-1 events, which contributes to the operational security enhancement.

The algorithm was tested using a simplified 107-bus version of the BIPS, and the results demonstrate significant benefits provided by the allocation of SVCs. Two solution strategies (Cases A and B) were compared with the original system configuration (Base Case), and their performance indicates a significant reduction in the Voltage Severity Index (VSI), decreasing from 428.5 in the Base Case to 166.8 in Case A and 196.2 in Case B. These results represent improvements of 61.1% and 54%, respectively, indicating a notable reduction in the magnitude of voltage violations.

Additionally, Case B, by incorporating the penalization of VSM violations, achieved substantial improvements in the voltage stability margin for the most critical contingencies compared to Case A, which considered only the minimization of voltage magnitude violations. Specifically, for the most critical contingency (line 104-1503), the VSM increased from 0.625% in the Base Case to 4.00% in Case B, representing a 540% improvement. The VSM can be expressed in terms of the additional load the system can safely withstand. The result obtained for Case B allows the system to handle 428 MW more than the Base Case and 254 MW more than Case A under the occurrence of the most critical line loss event.

Future research may address (*i*) the incorporation of uncertainties in load demand and renewable generation to better reflect real-world operational variability, potentially using stochastic or robust optimization frameworks, (*ii*) the extension and testing of the proposed VNS algorithm on larger-scale power systems, to assess its computational efficiency and scalability, and (*iii*) evaluation of the meta-heuristic's performance against exact optimization methods employing decomposition techniques.

REFERENCES

[1] M. Nadeem, K. Imran, A. Khattak, A. Ulasyar, A. Pal, M. Z. Zeb, A. N. Khan, and M. Padhee, "Optimal placement, sizing and coordination of FACTS devices in transmission network using whale optimization algorithm," *Energies*, vol. 13, no. 3, p. 753, Feb. 2020.

[2] L. Xue, T. Niu, S. Fang, and Z. Li, "Parameter optimization for var planning of systems with high penetration of wind power: An adaptive equivalent reduction method," *IEEE Trans. Sustain. Energy*, vol. 14, no. 4, pp. 1950–1963, Oct. 2023.

[3] R. Yan, N.-A.-Masood, T. K. Saha, F. Bai, and H. Gu, "The anatomy of the 2016 South Australia blackout: A catastrophic event in a high renewable network," *IEEE Trans. Power Syst.*, vol. 33, no. 5, pp. 5374–5388, Sep. 2018.

[4] *Análise Da Perturbação Do Dia 15/08/2023 às 08h30min*, Operador Nacional do Sistema Elétrico, Rio de Janeiro, Brazil, 2023. [Online]. Available: https://www.ons.org.br/AcervoDigitalDocumentosEPublicacoes/RAP%202023.08.15%2008h030min%20vers%C3%A3o%20final.pdf

[5] *Plano Da Operação Elétrica De Médio Prazo Do SIN—PAR/PEL 2024—Ciclo 2025–2029*, Operador Nacional do Sistema Elétrico, Brasília, Brazil, 2024.

[6] R. M. Mathur and R. K. Varma, *Thyristor-Based FACTS Controllers for Electrical Transmission Systems*. New York, NY, USA: Wiley, 2002.

[7] M. Rasheed, B. Hussain, A. S. Al-Sumaiti, and M. Abid, "Stability improvement of grid-connected DFIG wind farm with STATCOM compensated power network using RL-based coordinated transient controller," *IEEE Access*, vol. 13, pp. 116054–116068, 2025.

[8] M. Sarwar, M. Arshed, B. Hussain, M. Rasheed, H. Tariq, S. Czapp, S. Tariq, and I. A. Sajjad, "Stability enhancement of grid-connected wind power generation system using PSS, SFCL and STATCOM," *IEEE Access*, vol. 11, pp. 30832–30844, 2023.

[9] M. A. Kamarposhti, H. Shokouhandeh, I. Colak, S. S. Band, and K. Eguchi, "Optimal location of FACTS devices in order to simultaneously improving transmission losses and stability margin using artificial bee colony algorithm," *IEEE Access*, vol. 9, pp. 125920–125929, 2021.

[10] H. Amaris and M. Alonso, "Coordinated reactive power management in power networks with wind turbines and FACTS devices," *Energy Convers. Manage.*, vol. 52, no. 7, pp. 2575–2586, Jul. 2011.

[11] E. Ghahremani and I. Kamwa, "Optimal placement of multiple-type FACTS devices to maximize power system loadability using a generic graphical user interface," *IEEE Trans. Power Syst.*, vol. 28, no. 2, pp. 764–778, May 2013.

[12] R. W. Chang and T. K. Saha, "Maximizing power system loadability by optimal allocation of svc using mixed integer linear programming," in *Proc. IEEE PES Gen. Meeting*, Jul. 2010, pp. 1–7.

[13] X. Zhang, D. Shi, Z. Wang, J. Huang, X. Wang, G. Liu, and K. Tomsovic, "Optimal allocation of static var compensator via mixed integer conic programming," in *Proc. IEEE Power Energy Soc. Gen. Meeting*, Jul. 2017, pp. 1–5.

[14] M. N. U. Haq and X. Wang, "Optimal power loss minimization using static VAR compensator," in *Proc. Int. Conf. Control, Autom. Diagnosis (ICCAD)*, May 2024, pp. 1–6.

[15] P. Choudekar, S. K. Sinha, and A. Siddiqui, "Optimal location of SVC for improvement in voltage stability of a power system under normal and contingency condition," *Int. J. Syst. Assurance Eng. Manage.*, vol. 8, no. S2, pp. 1312–1318, Nov. 2017.

[16] D. Carrión, E. García, M. Jaramillo, and J. W. González, "A novel methodology for optimal SVC location considering N-1 contingencies and reactive power flows reconfiguration," *Energies*, vol. 14, no. 20, p. 6652, Oct. 2021.

[17] N. Yorino, E. E. El-Araby, H. Sasaki, and S. Harada, "A new formulation for facts allocation for security enhancement against voltage collapse," *IEEE Trans. Power Syst.*, vol. 18, no. 1, pp. 3–10, Feb. 2003.

[18] R. Minguez, F. Milano, R. Zarate-Minano, and A. J. Conejo, "Optimal network placement of SVC devices," *IEEE Trans. Power Syst.*, vol. 22, no. 4, pp. 1851–1860, Nov. 2007.

[19] Y. Chi, Y. Xu, and T. Ding, "Coordinated VAR planning for voltage stability enhancement of a wind-energy power system considering multiple resilience indices," *IEEE Trans. Sustain. Energy*, vol. 11, no. 4, pp. 2367–2379, Oct. 2020.

[20] Y. Chi, Y. Xu, and R. Zhang, "Many-objective robust optimization for dynamic VAR planning to enhance voltage stability of a wind-energy power system," *IEEE Trans. Power Del.*, vol. 36, no. 1, pp. 30–42, Feb. 2021.

[21] A. A. Eladl, M. I. Basha, and A. A. ElDesouky, "Techno-economic multi-objective reactive power planning in integrated wind power system with improving voltage stability," *Electric Power Syst. Res.*, vol. 214, Jan. 2023, Art. no. 108917.

[22] E. Davoodi, F. Capitanescu, M. I. Alizadeh, and L. Wehenkel, "A scalable var planning methodology to mitigate reactive power scarcity during energy transition," *IEEE Trans. Power Syst.*, vol. 40, no. 5, pp. 4182–4193, Sep. 2025.

[23] M. Eremia, A. Gole, and L. Toma, *Static VAr Compensator (SVC)*. Hoboken, NJ, USA: Wiley, 2016, ch. 5, pp. 271–338.

[24] P. Kundur, *Power System Stability and Control*. New York, NY, USA: McGraw-Hill, 1994.

[25] R. Z. Miano, "Optimal power flow with stability constraints," Ph.D. thesis, Dept. Elect. Eng., Universidad de Castilla-La Mancha, Ciudad Real, Spain, 2010.

[26] C. Taylor, *Power System Voltage Stability*. New York, NY, USA: McGraw-Hill, 1994.

[27] M. Eremia and M. Shahidehpour, Eds., *Handbook of Electrical Power System Dynamics: Modeling, Stability, and Control*. Hoboken, NJ, USA: Wiley, 2013.

[28] V. Ajjarapu and C. Christy, "The continuation power flow: A tool for steady state voltage stability analysis," *IEEE Trans. Power Syst.*, vol. 7, no. 1, pp. 416–423, Jan. 1992.

[29] M. K. Pal, "Voltage stability conditions considering load characteristics," *IEEE Trans. Power Syst.*, vol. 7, no. 1, pp. 243–249, Jan. 1992.

[30] M. A. M. Ramli and H. R. E. H. Bouchekara, "Solving the problem of large-scale optimal scheduling of distributed energy resources in smart grids using an improved variable neighborhood search," *IEEE Access*, vol. 8, pp. 77321–77335, 2020.

[31] *CEPEL, ANAREDE: Programa De Análise De Redes—Manual Do Usuário*, Rio de Janeiero, Brazil, 2023.

[32] P. Hansen and N. Mladenović, "Variable neighborhood search: Principles and applications," *Eur. J. Oper. Res.*, vol. 130, no. 3, pp. 449–467, May 2001.

[33] N. Mladenović and P. Hansen, "Variable neighborhood search," *Comput. Oper. Res.*, vol. 24, no. 11, pp. 1097–1100, 1997.

[34] W. F. Alves, "Proposição de sistemas-teste para análise computacional de sistemas de potência," Dept. Comput. Eng., Fluminense Federal Univ., Rio de Janeiro, Brazil, 2007.

[35] C. W. Taylor, G. Scott, and A. E. Hammad, "Static VAr compensator models for power flow and dynamic performance simulation," *IEEE Trans. Power Syst.*, vol. 9, no. 1, pp. 229–240, Jan. 1994.
[36] *Premissas, Critérios E Metodologia Para Estudos Elétricos*, Operador Nacional do Sistema Elétrico, Brasília, Brazil, 2023.
[37] C. E. C. Carrión, W. R. Faria, E. C. C. de Souza, E. Asada, and B. R. P. Junior, "Data set for a novel VNS-based algorithm for SVC allocation in the Brazilian interconnected power system," Tech. Rep., 2024. [Online]. Available: https://zenodo.org/records/14084641
[38] C. Coffrin and P. Van Hentenryck, "A linear-programming approximation of AC power flows," *INFORMS J. Comput.*, vol. 26, no. 4, pp. 718–734, Nov. 2014.
[39] C. Coffrin, R. Bent, K. Sundar, Y. Ng, and M. Lubin, "PowerModels. JL: An open-source framework for exploring power flow formulations," in *Proc. Power Syst. Comput. Conf. (PSCC)*, Jun. 2018, pp. 1–8.

CESAR E. C. CARRIÓN received the B.Eng. degree in electrical engineering from the National University of San Antonio Abad of Cusco, Cusco, Peru, in 2019, and the M.Sc. degree from the University of São Paulo (USP), São Carlos, Brazil, in 2023, where he is currently pursuing the Ph.D. degree in electrical engineering.

WANDRY R. FARIA received the B.Eng. degree from the Federal Institute of Goiás, Itumbiara, Brazil, in 2018, and the M.Sc. and Ph.D. degrees from the University of São Paulo, São Carlos, Brazil, in 2020 and 2024, respectively. He is currently a Postdoctoral Researcher with the University of São Paulo. His research interests include power system planning, operation, and markets.

ELLEN C. C. DE SOUZA received the B.Sc. degree in electrical engineering from the Federal University of Mato Grosso, Cuiabá, Brazil, in 2020, and the M.Sc. degree in electrical engineering from São Paulo School of Engineering (EESC), University of São Paulo (USP), São Carlos, Brazil, in 2023. She is currently pursuing the Ph.D. degree in electrical engineering with USP. Her research interests include renewable energy, power system operation planning, and power quality.

RODRIGO A. RAMOS (Senior Member, IEEE) received the B.Sc., M.Sc., and Ph.D. degrees in electrical engineering from the University of São Paulo, São Paulo, Brazil, in 1997, 1999, and 2002, respectively. He was a Visiting Professor with the University of New South Wales, Sydney, NSW, Australia, and a Visiting Associate Professor with the University of Waterloo, Waterloo, ON, Canada. He is currently an Associate Professor with the Department of Electrical and Computer Engineering, São Carlos School of Engineering, a unit of the University of São Paulo. He was an Associate Editor of IEEE TRANSACTIONS ON SUSTAINABLE ENERGY, IEEE TRANSACTIONS ON SMART GRID, and the *Journal of Modern Power Systems and Clean Energy*.

EDUARDO N. ASADA (Senior Member, IEEE) received the B.Eng. degree in electrical engineering and the M.Sc. and Ph.D. degrees from the University of Campinas (UNICAMP), Brazil, in 1997, 2000, and 2004, respectively. He is currently an Associate Professor with the Department of Electrical and Computer Engineering, São Carlos School of Engineering, University of São Paulo, Brazil. His research interests include state estimation, system planning, and applications of modern heuristic techniques to protection systems and smart grids.

BENVINDO R. PEREIRA JUNIOR received the B.S.Eng., M.Sc., and Ph.D. degrees from São Paulo State University, Ilha Solteira, Brazil. He is currently a Professor with the Department of Electrical and Computing Engineering, University of São Paulo, São Carlos, Brazil. His research interests include power system operation and planning, particularly developing mathematical models and metaheuristic applications for planning and operating electric power systems and energy markets.

Coordenação de Aperfeiçoamento de Pessoal de Nível Superior (CAPES) - ROR identifier: 00x0ma614